# Theoretical simulation of the photoassociation process for NaCs*

Zhang Chang-Zhe(张常哲), Zheng Bin(郑 斌), Wang Jun(王 军), and Meng Qing-Tian(孟庆田)†

*College of Physics and Electronics, Shandong Normal University, Jinan* 250014, *China*

(Received 7 July 2012; revised manuscript received 3 August 2012)

We investigate the two-step association process of NaCs using the time-dependent wave packet method. Ground state atoms can be photoassociated to the low vibrational levels of the ground state for an NaCs molecule by the two-step association. The time-dependent Schrödinger equation of the association process is solved within a three-state model and the wave packet is propagated with the "split operator-Fourier transform" scheme and the rotating-wave approximation (RWA). The vibrational population distribution of the ground state can be obtained by projecting the wave packet to every vibrational level of the ground state. The results not only show that for NaCs achievement of photoassociation production is accompanied by the photodissociation of the higher vibrational molecules, but also show that the vibrational distribution in lower vibrational levels of the ground state changes with the laser parameters.

**Keywords:** photoassociation, time-dependent wave packet method, NaCs

**PACS:** 34.50.Rk, 31.15.–P, 82.20.Bc, 82.30.Nr **DOI:** 10.1088/1674-1056/22/2/023401

## 1. Introduction

In recent years, with the development of ultrashort pulse laser techniques, many new phenomena of laser-molecule interaction have been observed and investigated, such as ac-Stark shift,[1,2] multiphoton ionization,[3–5] laser-induced continuum structure,[6–8] and photoassociation reaction.[9–11] As a reversed process of photodissociation, photoassociation has been studied both experimentally and theoretically. In 1995, Marvet and Dantus first investigated experimentally the formation of $Hg_2$ molecules with an ultrashort laser pulse.[12] The next year, Korolkov *et al.* studied the photoassociation reaction induced by a laser pulse with optimal parameters.[13] Nikolov and Ensher developed a two-step "R-transfer" method in 1999.[14] In 2004, four groups reported photoassociative production of three different ultracold heteronuclear diatomic molecules.[15–18] In 2011, Zhang Wei and Cong Shu-Lin *et al.* investigated the photoassociation (PA) dynamics implemented by a train of asymmetric slowly turned-on and rapidly turned-off (STRT) laser pulses and in the same year they also reported the PA dynamics of ultracold cesium atoms being controlled by varying the phase of the envelope (POE) $\phi$ and the period of the envelope $T_p$.[19,20]

In 2012, Lin Feng and Zhang Wei *et al.* studied the dependence of photoassociation probability on the cut-off position of the laser pulse.[21] Here, we study the two-step association process of the NaCs with the time-dependent quantum wave packet method which has been proved to be an effective and accurate method to investigate the interaction between molecules and an external field.[22–26] We choose NaCs for two reasons. First, NaCs has the largest measured dipole moment among all of the diatomic alkali molecules.[27] Second, Shaffer *et al.* have shown that cold Na and Cs have a substantial cross section for photoassociation.[28] Our scheme, depicted in Fig. 1, is conceptually similar to one proposed in Ref. [29]. In the first step, ground-state atoms are photoassociated to form long-range molecules in high vibrational levels of the $1^3\Pi$ state. Molecules photoassociated to the $1^3\Pi$ state cannot decay directly to the $X^1\Sigma^+$ state, because the Frank–Condon factors between the two states are very small in the regions we identified.[30] In the second step, the molecules are secondarily excited to the higher state. We have not identified the secondary state to which the molecules are excited. The density of states in this region is large and many states are possible. We offer one example, the $3^1\Pi$ state, which has the correct energy and good Frank–Condon factors with both the $1^3\Pi$ state and the $X^1\Sigma^+$ state. Finally, the molecules in low vibrational levels of the $X^1\Sigma^+$ state are achieved by spontaneous emission from the $3^1\Pi$ state.

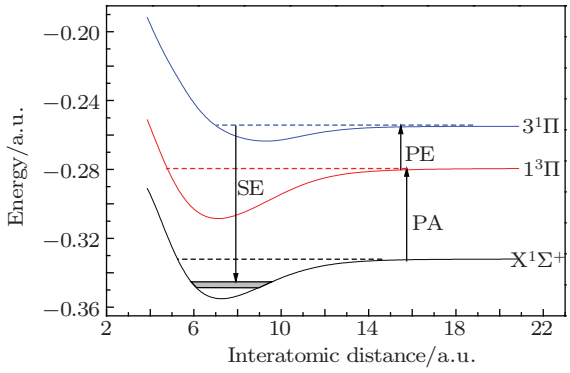



**Fig. 1.** (color online) Complete picture of ground state molecule production. Molecules are produced by photoassociation (PA) to vibrational levels of the $1^3\Pi$ state before being photo excited (PC) and finally undergoing spontaneous emission (SE) to the ground state. The unit a.u. is the abbreviation for atomic unit.

*Project supported by the National Natural Science Foundation of China (Grant No. 11074151) and the National Basic Research Program of China (Grant No. 2011CB808100).

†Corresponding author. E-mail: qtmeng@sdnu.ed.cn

© 2013 Chinese Physical Society and IOP Publishing Ltd 

In this paper, we investigate the two-step association process of NaCs using the time-dependent wave packet method. The remainder of this paper is organized as follows. Section 2 provides a brief review of the quantum wave packet method for photoassociation and photodissociation. The time-dependent Schrödinger equation and its solution with the scheme of wave packet propagation are then simply presented. The result and the discussion are given in Section 3. We conclude with a discussion of this work in Section 4.

## 2. Methodology

### 2.1. Time-dependent Schrödinger equation for the association

Within the Born–Oppenheimer approximation, the photoassociation process can be described by the time-dependent Schrödinger equation

$$\mathrm{i}\hbar\frac{\partial}{\partial t}|\psi(R,t)\rangle = [H_0 + W(t)]\,|\psi(R,t)\rangle\,, \tag{1}$$

where $H_0$ is the field-free Hamiltonian of the system and

$$W(t) = \mu E_0 f(t)\cos(\omega t + \phi) \tag{2}$$

is the laser-molecule interaction, $\mu$ the dipole moment operator and $f(t)$ is the shape of the pulse. $|\psi(R,t)\rangle$ is the time-dependent molecular wavefunction and the initial nuclear wavefunction, i.e., $|\psi(R,t=0)\rangle$ is described by the coherent Gaussian wave packet[31]

$$\psi(R) = \left(\frac{2}{\pi d_0}\right)^{1/4}\exp\left[\mathrm{i}kR - \left(\frac{R-R_0}{d_0}\right)^2\right], \tag{3}$$

where $d_0$ denotes the initial width of the wave packet, and $R_0$ is the initial internuclear distance between Na and Cs. The relative collision energy is given by

$$E_0 = \hbar^2(k^2 + 1/d_0^2)/(2m), \tag{4}$$

where $\hbar k$ and $m$ are the initial momentum and the reduced mass, respectively. In the calculation, the initial collision energy is 0.0077 eV, the initial width $d_0$ of the wave packet is taken to be $12a_0$ and $R_0$ is $16a_0$.

Generally we must use a very small time step to keep up with the fast oscillation of the laser frequency $\omega$, which involves a large amount of calculation. In order to simplify the calculation, we employ the RWA, then we can rewrite the time-dependent Schrödinger equation as[32]

$$\mathrm{i}\hbar\frac{\partial}{\partial t}\begin{pmatrix}\varphi_1\\ \varphi_2\\ \varphi_3\end{pmatrix} = \left\{\begin{pmatrix}T & 0 & 0\\ 0 & T & 0\\ 0 & 0 & T\end{pmatrix} + \begin{pmatrix}V_1 & \frac{1}{2}\hbar\Omega_1 & 0\\ \frac{1}{2}\hbar\Omega_1 & V_2-\hbar\omega_1 & \frac{1}{2}\hbar\Omega_2\\ 0 & \frac{1}{2}\hbar\Omega_2 & V_3-\hbar\omega_1-\hbar\omega_2\end{pmatrix}\right\}\begin{pmatrix}\varphi_1\\ \varphi_2\\ \varphi_3\end{pmatrix}, \tag{5}$$

where $\Omega = E(t)\mu(R)/\hbar$ is the Rabi frequency. $V_1, V_2, V_3$ denote the diabatic potential functions for $X^1\Sigma^+$, $1^3\Pi$, $3^1\Pi$ states, respectively.[33] With the rotating-wave approximation (RWA), we just need to consider the shape of the laser field $f(t)$ without regard to the laser frequency, so we can use a large time step to watch the motion of the wave packet and save computing time. By solving Eq. (5) we can get the wave packet in the low vibrational level of the $3^1\Pi$ state and then obtain the wave function of the $X^1\Sigma^+$state through spontaneous emission. The population of each state can be extracted from the norm of the nuclear wave packet $\varphi_i(R,t)$ $(i = 1,2,3)$, i.e.,

$$P_i(t) = \int_{R_1}^{R_2} \mathrm{d}R\,|\varphi_i(R,t)|^2, \tag{6}$$

where $R_1$ and $R_2$ define the range of inter-nuclear distances. We can also get the distribution of each vibrational level in the ground state from

$$P' = \left|\langle\phi_j(R,t)|\ \varphi(R,t)\rangle\right|^2, \tag{7}$$

where $\phi_j(R,t)$ $(j = 1, 2, 3, \ldots.)$ is the wave function of each vibrational level in the ground state.

### 2.2. The photodissociation of the molecule

Usually the NaCs molecules in the ground electronic state are populated both high-vibrationally and low-vibrationally because of spontaneous emission and the influence of the first laser pulse. In order to obtain the molecules only in low vibrational levels, noticing that there is a repulsive excited state $1^3\Sigma^+$ which couples closely with the $X^1\Sigma^+$ state, we can use a laser beam with low frequency to dissociate the molecules in high vibrational levels. As a result, the molecules which mainly populate low vibrational levels of the $X^1\Sigma^+$ state are obtained. Under RWA, the time-dependent Schrödinger equation for the system can be written as

$$\mathrm{i}\hbar\frac{\partial}{\partial t}\psi(R,t) = \boldsymbol{H}\psi(R,t), \tag{8}$$

with Hamiltonian $\boldsymbol{H} = \boldsymbol{T} + \boldsymbol{V}$, $\boldsymbol{T}$ the kinetic matrix, $\boldsymbol{V}$ the potential matrix, and

$$\psi(R,t) = \begin{pmatrix}\psi_1\\ \psi_2\end{pmatrix}, \tag{9}$$

$$\boldsymbol{T} = -\frac{\hbar^2}{2m}\frac{\partial}{\partial R^2}\begin{pmatrix}1 & 0\\ 0 & 1\end{pmatrix},$$

$$\boldsymbol{V} = \begin{pmatrix} V_1 & \frac{1}{2}\mu_{12}E \\ \frac{1}{2}\mu_{21}E & V_2 - \hbar\omega \end{pmatrix}, \tag{10}$$

where $m$ is the reduced mass, $V_1$, $V_2$ the diabatic potential functions for the ground and excited states and $\mu$ is the same as before. In Eq. (9), $\psi_1$ and $\psi_2$ represent the time-dependent nuclear wave functions in the lower and upper states, respectively, which are obtained by the following wave packet propagation scheme.

Consider a small time interval $\Delta t$. Using the split-operator technique, the canonical solution of Eq. (8) can be written up to second-order approximation as[34]

$$\Psi(R,t_0+\Delta t) \approx U_V^{1/2} U_T U_V^{1/2} \Psi(R,t_0), \tag{11}$$

where $\psi(R,t_0)$ is the wave packet at the initial time $t_0$, and

$$U_T = \exp\left[-\frac{\mathrm{i}\Delta t}{\hbar}T\right], \quad U_V = \exp\left[-\frac{\mathrm{i}\Delta t}{\hbar}V(R,t_0)\right] \tag{12}$$

are called the kinetic- and potential-energy evolution operators, respectively. After propagating $n$ steps, the wave function assumes the form

$$\Psi(R,t_0+n\Delta t) \approx \left[\prod_{k=0}^{n-1} U_T U_V (R,t_0+k\Delta t)\right] \Psi(R,t_0). \tag{13}$$

The dissociation probability in each channel can be calculated from the probability flux of the wave function at the nuclear separation $R_\mathrm{d}$,

$$J_i(t) = \frac{\hbar}{m}\,\mathrm{Im}\left[\psi_i^*(R,t)\frac{\partial\psi_i(R,t)}{\partial R}\right]_{R=R_\mathrm{d}}. \tag{14}$$

If we write the outgoing wave-packet in terms of a real amplitude $A$ and a real phase $\phi$, i.e.,

$$\psi_i(R,t) = A_i(R,t)\exp[\mathrm{i}\phi_i(R,t)], \tag{15}$$

then the current density can be written as[35]

$$J_i(t) = \frac{|A_i(R,t)|^2}{m}\nabla\phi_i(R,t). \tag{16}$$

The dissociation yield of fragments, $D$, is given by the following integration along the nuclear flux direction at $R_\mathrm{d}$

$$D(t) = \int_0^t \mathrm{d}t' J_i(R_\mathrm{d},t'). \tag{17}$$

## 3. Results and discussion

In the two-step association scheme, the effect of the first laser pulse must leave an impression in the ground state. Figure 2(a) shows the vibrational population distributed mainly around the vibrational level $\upsilon > 60$ after the first pulse. This high vibrational distribution is caused by the excitation of the initial wave packet in the form of Eq. (3) and the decay of the wave packet to the $X^1\Sigma^+$ state induced by the first pulse. The vibrational distribution after the two-step association is shown in Fig. 2(b). Obviously since the population in higher vibrational levels has been dissociated through the repulsive excited state, the population in the ground state is just in lower vibrational levels.

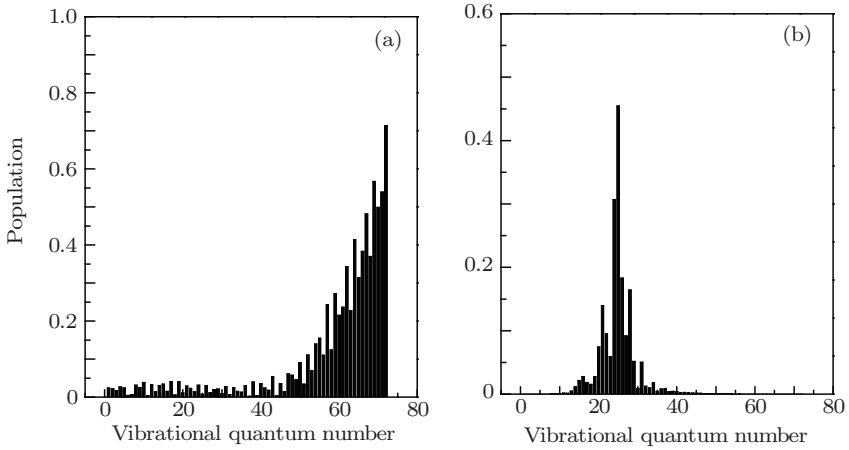



**Fig. 2.** (a) Population in each vibrational level of the ground state after the first laser pulse; (b) Distribution after the two-step association.

The adiabatic potential curves of dissociation process and the dissociation probability as a function of time are shown in Fig. 3 and Fig. 4, respectively. In Fig. 3, there are two dissociation channels, the upper channel (red line) and the lower one (black line). We can see a plateau region of the dissociation probability via the lower dissociation channel (red line in Fig. 4), which can be explained by the evolution of the wave packet on the potential curves. The wave packet is pumped onto the excited state. When it reaches the location of the avoided crossing, coming from the left turning point, part of it transmits across this region to the lower potential curve and dissociates. Then the wave packet moves forward continuously along the potential well. It goes back after arriving at the right-hand-side turning point and completes the first pe-

riod. In the next period, the wave packet moves along the upper potential curve and dissociates again when it goes through the avoided crossing point. The dissociation probability via the upper channel (black line in Fig. 4) is monotonously increasing instead of increasing with plateau region because the remaining wave packet after the first dissociation period does not have enough energy to run out of the potential well and dissociate again.

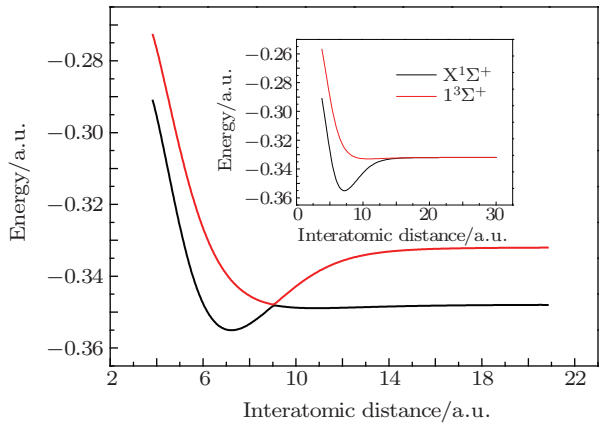



**Fig. 3.** (color online) Adiabatic and diabatic (lines in the inset) potential curves for the $X^1\Sigma^+$ and $1^3\Sigma^+$ states of NaCs.

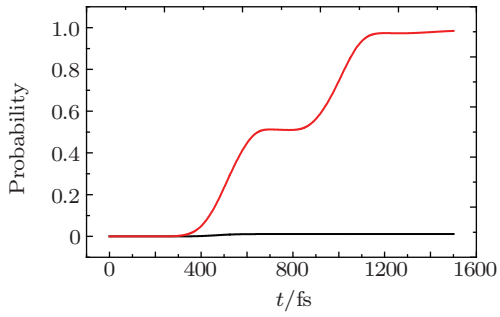



**Fig. 4.** (color online) Dissociation probability as a function of time.

Having obtained the production of NaCs in low vibrational levels above, we now turn to the changes of population distribution with changing laser parameters. First, the distribution in the ground state changing with the laser frequency is studied. As shown in Fig. 5, with the increase of the pulse frequency, the center of the vibrational population distribution shifts to higher vibrational levels. This phenomenon can be explained thus: with the increase of the laser frequency, the wave packet is pumped onto the second excited electronic state, and the higher vibrational levels can be populated, so the population in the ground state formed by the spontaneous emission from the $3^1\Pi$ state concentrates upon the higher vibrational levels due to the influence of the Franck–Condon factor.

Second, we are also interested in the variation of the population with the pulse duration. From above we know that the photoassociation process is related to the selectivity of the vibrational states. Obviously this selectivity is relevant to the duration of pulse used. The uncertainty relation $\Delta E \cdot \Delta t \geq \hbar/2$ shows that with the increase of the pulse duration, the uncertainty of the energy becomes less. As a result, more vibrational levels are in resonance and excited states, which leads to the reduction of the state selectivity. As shown in Fig. 6, when the pulse duration is 80 fs, the vibrational population distributes mainly in $\upsilon = 25 \sim 35$, and the center is located at $\upsilon = 30$, while the distribution of the vibrational population is mostly in the range of $\upsilon = 20 \sim 40$ and $\upsilon = 15 \sim 45$ when the pulse duration is 60 fs and 40 fs, respectively.

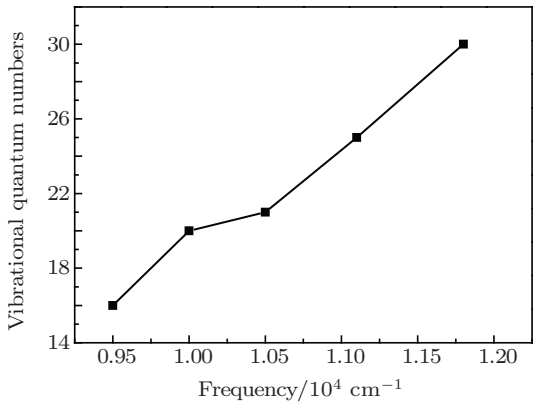



**Fig. 5.** Central vibrational level of the population distribution in ground state changes with the laser frequency.

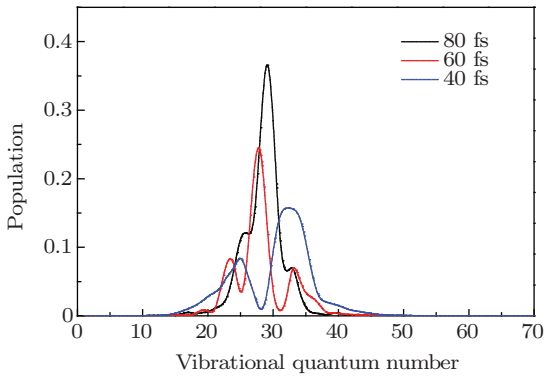



**Fig. 6.** (color online) The population distribution in the $X^1\Sigma^+$ state for pulse durations 80 fs, 60 fs, and 40 fs.

Third, we investigate the population distribution at different delay times between two laser beams as shown in Figs. 7(a)–7(c). Figure 7(a) displays the vibrational distribution in the $X^1\Sigma^+$ state for the delay time 0 fs; figures 7(b) and 7(c) exhibit the vibrational distribution in the $X^1\Sigma^+$state when the delay time is 60 fs and 110 fs, respectively. The results show that the main distribution area of the population shifts from the high vibrational levels to the low vibrational levels gradually with the increase of the delay time. This phenomenon can be elucidated by the evolution of the wave packet

in the $1^3\Pi$ state. The wave packet is pumped onto the $1^3\Pi$ state by the first laser, and then it will move along the potential curve from high vibrational levels to low vibrational levels before the second laser works. With the delay time increasing, the wave packet moves to lower vibrational levels and then is excited to related lower vibrational levels of the $3^1\Pi$ state by the second laser pulse. Consequently, the population in lower vibrational levels is produced by spontaneous emission.

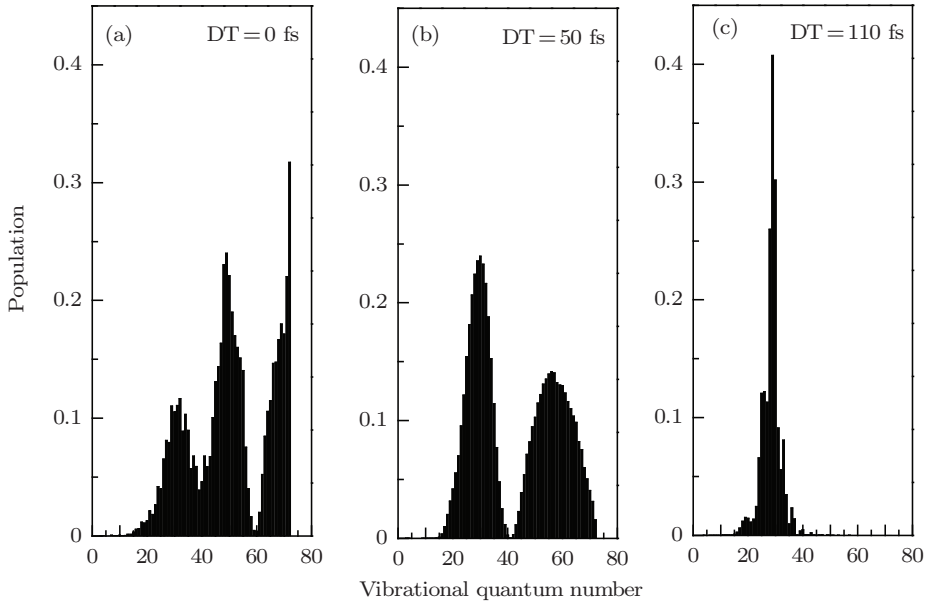



**Fig. 7.** The distribution in the $X^1\Sigma^+$ state for different delay time. The distribution is abbreviated to DT in the figure.

## 4. Summary

In this paper we investigated the two-step association process of NaCs using the time-dependent wave packet quantum dynamics on accurate *ab initio* PECs. In order to achieve the NaCs molecules most populated in low vibrational levels, we used a laser beam to dissociate the molecules in high vibrational levels of the $X^1\Sigma^+$ state. The results show that the molecules in low vibrational levels of the ground state can be produced through the association and dissociation process. The vibrational population distribution in the ground state changes with the laser parameters. We noticed that the center of the vibrational distribution in the $X^1\Sigma^+$ state shifts to higher vibrational levels with increasing laser frequency. By analyzing the changes of population distribution with different laser duration, we also found that the longer the laser duration, the better the state selectivity. Finally, the influence of the delay time, one of the important parameters of laser pulses, on photoassociation was studied. The result shows that the main distribution area of the population gradually shifts from high vibrational levels to low vibrational levels with the increase of delay time. These results obtained from our work are probably helpful for exploring the formation of the ultracold molecules and can provide some useful information for the relevant experiments.

## References

[1] Degenhardt C, Stoehr H, Sterr U and Riehle F 2004 *Phys. Rev.* A **70** 023414
[2] Stapelfeldt H, Sakai H, Constant E and Corkum P B 1997 *Phys. Rev. Lett.* **79** 2787
[3] Zhang L D, Wei J, Jiang Y Y, Fang L, Zhang S D, Guo W Y and Cai J Y 1998 *Chin. Phys.* **7** 271
[4] Niu D W, Li H Y, Luo X L, Liang F, Cheng S and Li A L 2006 *Chin. Phys.* **15** 1511
[5] Wickenhauser M, Tong X M, Arbó D G, Burgdörfer J and Lin C D 2006 *Phys. Rev.* A **74** 041402
[6] Li G X, Huang G M and Peng J S 1998 *Chin. Phys.* **7** 422
[7] Eramo R, Cavalier S, Fini L, Matera M and Dimauro L F 1997 *J. Phys.* B **30** 3789
[8] Faucher O, Hertz E, Lavorel B, Chaux R, DreierT, Berger H and Charalambidis D 1999 *J. Phys.* B **32** 4485
[9] Sage J M, Sainis S, Bergeman T and DeMille D 2005 *Phys. Rev. Lett.* **94** 203001
[10] Fioretti A, Comparat D, Crubellier A, Dulieu O, Masnou-Seeuws F and Pillet P 1998 *Phys. Rev. Lett.* **80** 4402
[11] Lin F, Zhang W, Zhao Z Y and Cong S L 2012 *Chin. Phys.* B **21** 073203
[12] Zhang H S, Ji Z H, Yuan J P, Zhao Y T, Ma J, Wang L R, Xiao L T and Jia S T 2011 *Chin. Phys.* B **20** 123702
[13] Marvet U and Dantus M 1995 *Chem. Phys. Lett.* **219** 161
[14] Korolkov M V, Manz J, Paramonov G K and Schmidt B 1996 *Chem. Phys. Lett.* **260** 604
[15] Nikolov A N, Ensher J R, Eyler E E, Wang H, Stwalley W C and Gould P L 1999 *Phys. Rev. Lett.* **84** 246
[16] Haimberger C, Kleinert J, Bhattacharya M and Bigelow N P 2004 *Phys. Rev.* A **70** 021402
[17] Mancini M W, Telles G D, Caires A R L, Bagnato V S and Marcassa L G 2004 *Phys. Rev. Lett.* **92** 133203
[18] Kerman A J, Sage J M, Sainis S, Bergeman T and DeMille D 2004 *Phys. Rev. Lett.* **92** 153001

[19] Wang D, Qi J, Stone M F, Nikolayeva O, Wang H, Hattaway B, Gensemer S D, Gould P L, Eyler E E and Stwalley W C 2004 *Phys. Rev. Lett.* **93** 243005
[20] Zhang W, Wang G R and Cong S L 2011 *Phys. Rev.* A **83** 045401
[21] Zhang W, Zhao Z Y, Xie T, Wang G R, Huang Y and Cong S L 2011 *Phys. Rev.* A **84** 053418
[22] Meng Q T, Yang G H, Sun H L, Han K L and Lou N Q 2003 *Phys. Rev.* A **67** 063202
[23] Yu J, Wang S M, Yuan K J and Cong S L 2006 *Chin. Phys.* **15** 1996
[24] Wang J, Liu F, Yue D G, Zhao J, Xu Y, Meng Q T and Liu W K 2010 *Chin. Phys.* B **19** 123301
[25] Lu R F, Zhang P Y and Han K L 2008 *Phys. Rev.* E **77** 066701
[26] Meng Q T, Yang G H and Han K L 2003 *Int. J. Quantum Chem.* **95** 30
[27] Igel-Mann G, Wedig U, Fuentealba P and Stoll H 1986 *J. Chem. Phys.* **84** 5007
[28] Shaffer J P, Chalupczak W and Bigelow N P 1999 *Phys. Rev. Lett.* **82** 1124
[29] Band Y B and Julienne P S 1995 *Phys. Rev.* A **51** R4317
[30] Haimberger C 2008 *Photoassociation of Ultracold* NaCs (Ph. D. thesis) University of Rochester, Rochester, New York
[31] Niu Y Y, Wang R, Liu L and Cong S L 2007 *Chin. Phys. Lett.* **24** 3400
[32] Whaley K B and Light J C 1984 *Phys. Rev.* A **29** 1188
[33] Aymar M and Dulieu O 2007 *Mol. Phys.* **105** 1733
[34] Feit M D, Fleck J A and Steiger A 1982 *J. Comput. Phys.* **47** 412
[35] Feuerstein B and Thumm U 2003 *Phys. Rev.* A **67** 043405